

High-resolution studies of sulfur- and selenium-related donor centers in silicon

E. Janzén,* R. Stedman, G. Grossmann, and H. G. Grimmeiss
 Department of Solid State Physics, University of Lund, Box 725, S-220 07 Lund, Sweden
 (Received 8 August 1983; revised manuscript received 24 October 1983)

High-resolution infrared absorption and photoconductivity spectra of several S- and Se-related donor centers in silicon are presented. These include isolated, probably substitutional, impurities and impurity pairs, as well as more complex centers. The spectra of the isolated impurities are consistent with T_d symmetry and those of impurity pairs with D_{3d} symmetry. The binding energies of excited states are recalculated in accordance with effective-mass theory. The results agree better with experiments than previously published calculations. The spectra are discussed in detail with emphasis on valley-orbit splittings of excited states in T_d and D_{3d} symmetry.

I. INTRODUCTION

Sulfur and selenium give rise to various donor centers in silicon. These may involve one, two, or more impurity atoms, and may be either neutral or ionized. For some centers our knowledge is quite extensive,^{1,2} at least experimentally, while for others it is less certain. One of the most important sources of information about such centers is their excitation spectra, since well-resolved excited states may reveal much of the microscopic structure of defects. The quality of spectra has gradually improved as sample materials and experimental methods have developed. The spectra presented here exhibit considerable detail for several centers related to S and Se. They are infrared-absorption spectra and photoconductivity spectra recorded with a Fourier-transform infrared spectrometer, representing results for a large number of samples prepared under varying conditions. Binding energies of states have been derived from spectra, and compared with new calculations based on the effective-mass approximation. This approximation is poor for the lowest donor levels, but even there it provides a reference in assigning spectral lines when augmented with a splitting into multivalley components in accordance with local symmetry.

Designations for the various centers vary in the literature. The labels we use here are shown in Figs. 1 and 2, which illustrate the ground-state binding energies of several centers. The superscript of the label gives the state

of ionization when the donor is occupied, while a subscript indicates when the donor is a pair of atoms (2) or more complex (c). Thus D^0 and D^+ are the neutral and singly ionized versions of an isolated D atom which occupies a tetrahedral, probably substitutional, site. D_2^0 and D_2^+ are corresponding versions of a pair, while $D_c(X_i)$ are more complex D -related centers about which little is known.

Calculations of excited-state energies for donors in silicon were made several years ago by Faulkner³ in accordance with effective-mass theory (EMT). An extended version of the same variational method which has been used here is briefly described in Sec. III. It is shown in Sec. IV that these calculations agree well with the observations reported here for p -like states of neutral donor centers. This is expected, since the orbitals of such states lie in regions where the potential of the donor center varies slowly enough over a unit cell for the effective-mass approximation to be valid. But for s states—particularly $1s$ states—the central part of the potential gives rise to a significant interaction between the six “valley” states that are degenerate in the EMT, splitting them into components of lower degeneracy in accordance with the local symmetry of the donor center. The s states of D^0 are treated in Sec. V, and those of D_2^0 in Sec. VI. In Sec. VII the complex D_c centers are discussed, with reference to recent results on thermal donors^{4,5,6} and magnesium-doped

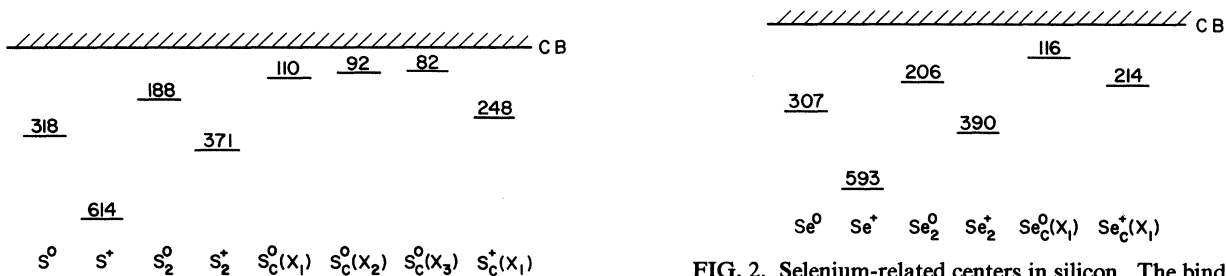


FIG. 1. Sulfur-related centers in silicon. $S_c^+(X_1)$, $S_c^0(X_2)$, and $S_c^0(X_3)$ are sulfur-related complexes not observed previously (see also, however, Refs. 29 and 30). The binding energies of all centers are taken from this paper and are similar to those found in the literature (Refs. 8, 15, 22, 23, 25, 30, 31, and 37–44).

FIG. 2. Selenium-related centers in silicon. The binding energies of $Se_c^0(X_1)$ and $Se_c^+(X_1)$ complexes are taken from Ref. 28. The binding energies for the other centers are taken from this paper and are in good agreement with those found in the literature (Refs. 8, 28, 31, and 45–50), except for the Se^+ center for which our value is 4 meV less than that reported in Ref. 28.

silicon.⁷ Finally, in Secs. VIII and IX the ionized centers are treated. Since the electron is more tightly bound in these centers, the effect of local symmetry in valley-orbit splitting becomes more pronounced.

II. SAMPLE PREPARATION AND EXPERIMENTAL METHODS

The silicon wafers used in investigating the neutral donor centers were of float-zone material with extremely low oxygen and carbon content. Before the introduction of S or Se by diffusion the carrier concentration was $4 \times 10^{12} \text{ cm}^{-3}$, and was due to phosphorus. Each wafer, 350–2000 μm thick, was polished and etched and put into an ampoule together with a mixture of the dopant and silicon powder, after which the ampoule was filled with argon and sealed. A considerable number of different samples were prepared by varying the vapor pressure of the dopant (see Ref. 8), the diffusion temperature, and the diffusion time. Diffusion temperatures were between 825 and 1100°C for sulfur and between 960 and 1200°C for selenium. Diffusion times were between 8 and 260 h. It was found that high vapor pressure and high diffusion temperature favored the formation of pairs (i.e., D_2), although pairs did form even when the sulfur concentration was as low as 10^{13} cm^{-3} . The effect of vapor pressure on the formation of pairs was stronger for selenium than for sulfur. After diffusion, the wafers were polished and etched again. Samples for photoconductivity measurements were furnished with alloyed (Au/Sb) contacts and mounted stress free on standard TO-5 holders. All samples were mounted at one edge with weak adhesive to ensure freedom from stress.

Samples for the investigation of the D_2^+ centers were made in a similar manner, but starting with p -type material (resistivity of 0.3 $\Omega \text{ cm}$). Some samples were made by the epitaxial technique described in Ref. 9.¹⁰

The spectral measurements were performed on a Fourier-transform spectrometer (Nicolet 8000 HV), and were of both absorption and photoconductivity. In the latter method bound states are detected by photothermal excitation, i.e., photoexcitation followed by thermal ionization. The two types of measurement complement one another in that absorption covers the whole spectrum of a center, whereas the generally more sensitive photoconductivity method gives details of the higher excited states. To obtain narrow lines it is necessary to use low temperatures, and at these temperatures only excited states fairly close to the conduction band can be thermally ionized. The lower sensitivity of absorption measurements is due to the fact that significant structure is seen against the relatively noisy background of fluctuations in the photon flux through the sample, whereas in a photoconductor little of this flux produces a signal.

III. BINDING ENERGIES CALCULATED IN THE EFFECTIVE-MASS APPROXIMATION

Faulkner³ calculated the energy levels of the effective-mass Hamiltonian for a series of values of the effective-mass ratio m_t/m_l . His method was based on the

Rayleigh-Ritz variational principle, taking ellipsoidal hydrogenic wave functions as a basis set. Owing to the anisotropy of the conduction band, only parity and the projection of angular momentum l along the principal axis of the prolate spheroid m remain good quantum numbers. States were accordingly classified as s -like when their parity was even (l even) and $m=0$, and as p -like when their parity was odd (l odd) and $m=0$ (p_0 -like) or $m=\pm 1$ (p_{\pm} -like). In each case, the calculation was performed using basis functions corresponding to three values of angular momentum l and for each l up to six values of the principal quantum number n . This yielded a secular problem of dimension $3 \times 6 = 18$. The eigenvalues were then determined variationally as functions of a parameter β determining the "eccentricity" and a set of parameters α_l , one for each l value, determining the degree of localization of the basis functions.

A limitation of Faulkner's results for our purposes is that only the nine lowest s -, p_0 -, and p_{\pm} -like states were calculated, and that the binding energies are liable to be somewhat inaccurate for the higher levels because a rather limited number of basis functions (3×6) was included in the computation. Experiments are now beginning to resolve these higher states, and information on d -like states may also become important for the interpretation of data (cf. Sec. V). Furthermore, the results presented for silicon were obtained from curves interpolating between results calculated for a set of different effective-mass ratios. In order to reduce the theoretical uncertainty below that of experiment, we repeated the calculation for the specific case of silicon, i.e., using the effective masses defined by $m_t/m=0.1905$ and $\gamma=m_t/m_l=0.2079$ together with the value 11.40 obtained by Faulkner for the static dielectric constant.

The basis set was extended until the results had converged to within about 10^{-3} meV, which required us to include up to six values of l and, for each l , up to 15 values of n , i.e., to deal with up to 90×90 Hamiltonian matrices and with up to seven variational parameters. The calculations were carried out along the lines given by Faulkner and for further details we refer the reader to Ref. 3. For the larger values of n and l , however, the series expansion of the Laguerre polynomials [Eq. (2.8) of Ref. 3] becomes numerically inconvenient, and the radial integrals were instead evaluated recursively, using the recurrence relations given, e.g., by Arfken.¹¹ The minima of the eigenvalues were found using the minimization routine VA10A of the Harwell Subroutine Library. Our results, which also include d -like states, i.e., states with even parity and $m=\pm 1$ (d_{\pm}) or $m=\pm 2$ ($d_{\pm 2}$), are given in Table I (see Ref. 12). There we also give the binding energies of the lowest f -like states—odd parity and $m=\pm 2$ and ± 3 —below which no further bound states are expected. It may be noted that these lowest f -like states, such as the lowest states of the other series, are strikingly "pure," i.e., the variational wave function can very accurately be represented by a single trial basis function.

While our values differ only slightly from Faulkner's, i.e., by less than 0.1 meV, we find a significantly better agreement with experiment in all cases where the EMT may be expected to be valid. The remaining discrepancies

TABLE I. EMT binding energies in millielectron volts for silicon obtained in the present work.

<i>s</i> -like states	1 <i>s</i>	2 <i>s</i>	3 <i>s</i>	3 <i>d</i> ₀	4 <i>s</i>	4 <i>d</i> ₀	
	31.262	8.856	4.777	3.751	2.911	2.141	
	5 <i>s</i>	5 <i>d</i> ₀	5 <i>g</i> ₀	6 <i>s</i>	6 <i>d</i> ₀	6 <i>g</i> ₀	7 <i>s</i>
	1.929	1.546	1.458	1.281	1.160	1.045	0.911
<i>p</i> ₀ -like states	2 <i>p</i> ₀	3 <i>p</i> ₀	4 <i>p</i> ₀	4 <i>f</i> ₀	5 <i>p</i> ₀	5 <i>f</i> ₀	
	11.492	5.485	3.309	2.339	2.235	1.630	
	6 <i>p</i> ₀	6 <i>f</i> ₀	6 <i>h</i> ₀	7 <i>p</i> ₀	7 <i>f</i> ₀	7 <i>h</i> ₀	
	1.510	1.241	1.102	1.004	0.980	0.842	
<i>p</i> _± -like states	2 <i>p</i> _±	3 <i>p</i> _±	4 <i>p</i> _±	4 <i>f</i> _±	5 <i>p</i> _±	5 <i>f</i> _±	
	6.402	3.120	2.187	1.894	1.449	1.260	
	6 <i>p</i> _±	6 <i>f</i> _±	6 <i>h</i> _±	7 <i>p</i> _±	7 <i>f</i> _±	7 <i>h</i> _±	
	1.070	1.002	0.886	0.822	0.750	0.676	
<i>d</i> _± -like states	3 <i>d</i> _±	4 <i>d</i> _±	5 <i>d</i> _±	5 <i>g</i> _±	6 <i>d</i> _±	6 <i>g</i> _±	
	3.874	2.338	1.617	1.413	1.194	0.991	
	7 <i>d</i> _±	7 <i>g</i> _±	7 <i>i</i> _±	8 <i>d</i> _±	8 <i>g</i> _±	8 <i>i</i> _±	
	0.922	0.768	0.739	0.713	0.618	0.594	
<i>d</i> _{±2} -like states	3 <i>d</i> _{±2}	4 <i>d</i> _{±2}	5 <i>d</i> _{±2}	5 <i>g</i> _{±2}	6 <i>d</i> _{±2}	6 <i>g</i> _{±2}	
	2.632	1.587	1.267	1.098	0.887	0.810	
	7 <i>d</i> _{±2}	7 <i>g</i> _{±2}	7 <i>i</i> _{±2}	8 <i>d</i> _{±2}	8 <i>g</i> _{±2}	8 <i>i</i> _{±2}	
	0.707	0.674	0.610	0.556	0.533	0.475	
<i>f</i> -like states	4 <i>f</i> _{±2}		4 <i>f</i> _{±3}				
	1.893		1.421				

are within experimental accuracy, which at present is about ± 0.01 meV. Thus there was no reason to question the accuracy of the input parameters. In what follows we will refer to our new values as "EMT energies."

IV. *p*-LIKE STATES OF D^0 and D_2^0

The energy-level scheme of an isolated substitutional chalcogen donor is shown in Fig. 3, based on the EMT for a single conduction-band minimum modified by valley-orbit splitting in tetrahedral symmetry. Selection rules for optical transitions in this model are summarized there. Experimental results for the Se^0 center are shown in Fig. 4, with assignments according to final states in the scheme of Fig. 3. Figure 4 also compares an absorption spectrum with a photoconductivity spectrum, and the emphasis on higher excited states in the latter, which was mentioned in the Introduction, is clearly apparent. The $1s(T_2)$ and $2s(T_2)$ lines of the Se^0 center are seen as dips in the photoconductivity spectrum, due to absorption of photons in exciting states that are not subsequently ionized thermally. Note that the $2p_0$ line is seen as a peak although $2p_0$ is

deeper than $2s(T_2)$, which indicates a difference in the relative strength of recombination and ionization for these states. The structure from 320 meV upwards is due to Fano resonances, where the excitation of a bound electronic state, together with an intervalley phonon, interferes with the excitation to the overlapping electronic continuum.¹³⁻¹⁵ A similar absorption spectrum for the S^0 center is shown in Fig. 5.

The energy of *p*-like states relative to the ionization limit are notably insensitive to the nature of the defect. Figure 6 shows photoconductivity spectra for the upper states of the S^0 , Se^0 , S_2^0 , and Se_2^0 centers and it is obvious that the line spectra are almost identical, relative to the respective ionization limits. Relative heights differ somewhat, probably due to temperature differences.

The essential features of the spectra shown in Figs. 4-6 are identical to those observed for shallow group-V donors^{16,17} in silicon and to what is predicted by the EMT. The results are summarized in Table II and compared with EMT calculations. The ionization limit—i.e., the binding energy of the ground state—has been obtained by adding the effective-mass binding energy of the $3p_{\pm}$

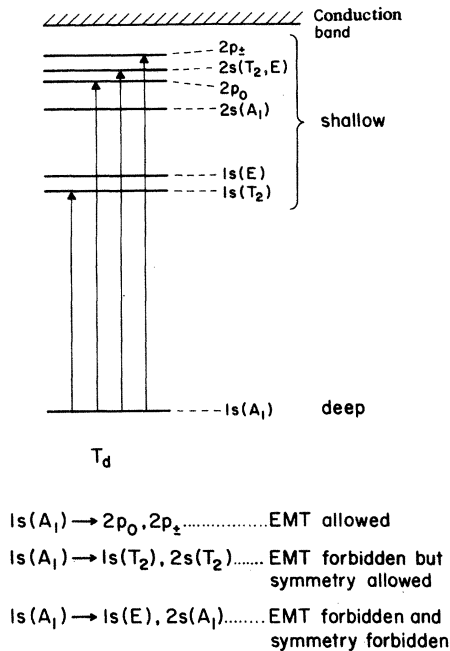


FIG. 3. Lowest part of the energy spectrum of a substitutional donor in silicon. Symmetry-allowed transitions are marked with arrows.

state, 3.12 meV, to the observed excitation energy, $1s(A_1) \rightarrow 3p_{\pm}$. The accuracy of the experimental values in Table II is better than 0.02 meV except for those marked by Refs. a and b. The latter are either broadened or partly obscured by stronger lines (Ref. b) or derived from Fano replicas (Ref. a); see Ref. 14. The largest deviation from the EMT value is for the $2p_0$ state of the Se_2^0 center, but as this is the deepest p state, it is also the one most susceptible to influence from the region close to the center where the potential does not agree with the EMT assumptions. Note that, e.g., our EMT value for the $6p_{\pm}$ state agrees notably better with experiment than Faulkner's. Compare, also, the shallow donors presented in Table II of Ref. 17.

From Fig. 6 there is obviously at least one further excited state above $6p_{\pm}$, with a binding energy close to 0.85 meV. Skolnick *et al.*¹⁸ found two lines above $6p_{\pm}$ for phosphorus, one at 0.85 meV and a weaker one at 0.96 meV below the conduction band. Furthermore, Pajot *et al.*¹⁶ have reported a state at 0.88 meV in phosphorus. The calculated energy of $7p_{\pm}$ is 0.82 meV and that of $6h_{\pm}$ is 0.89 meV (see Table I), and the intensities estimated rather crudely on the basis of our EMT calculation are similar. We thus cannot at present make any definite assignment for our peak, but nevertheless we label it $7p_{\pm}$, as this alternative seems more likely.

V. s -LIKE STATES OF D^0

Properly symmetrized states are obtained as linear combinations of the EMT states associated with each of the six equivalent conduction-band minima of silicon. For the s -like states in tetrahedral symmetry one finds a singlet (A_1), a doublet (E), and a triplet (T_2).¹⁹ When inter-

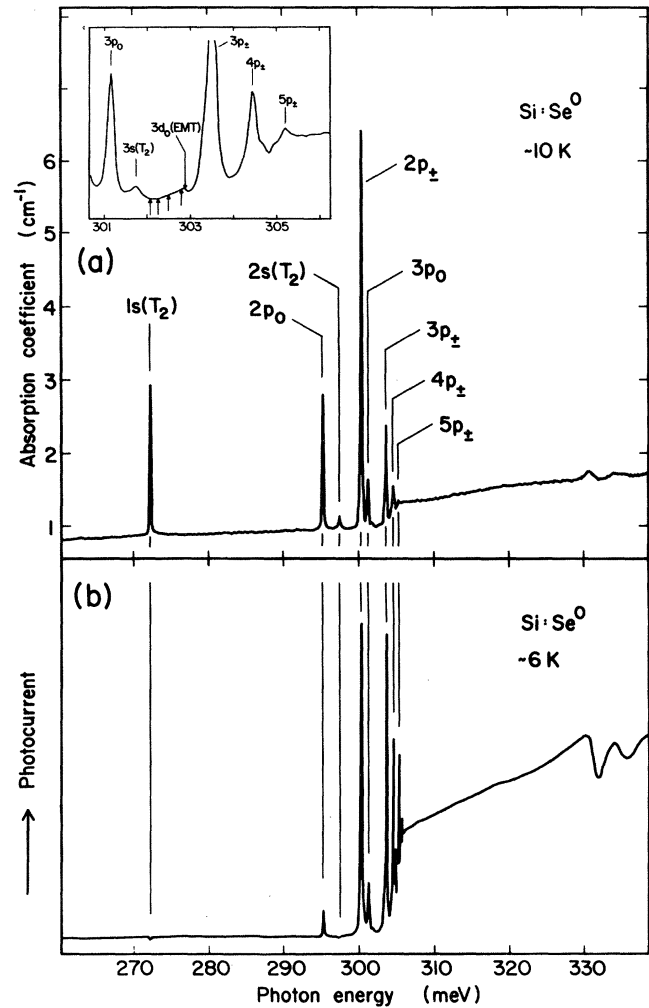


FIG. 4. Line spectra of $Si:Se^0$. (a) Absorption spectrum of selenium-doped silicon with approximately $3 \times 10^{16} \text{ cm}^{-3}$ Se atoms; the resolution is 0.12 meV. The arrows in the inset indicate the energy positions of the four small peaks in the left-hand inset of Fig. 6(a). (b) Photoconductivity spectrum of selenium-doped silicon with approximately $3 \times 10^{15} \text{ cm}^{-3}$ Se atoms. The electric field is less than 10 V/cm; the resolution is 0.03 meV.

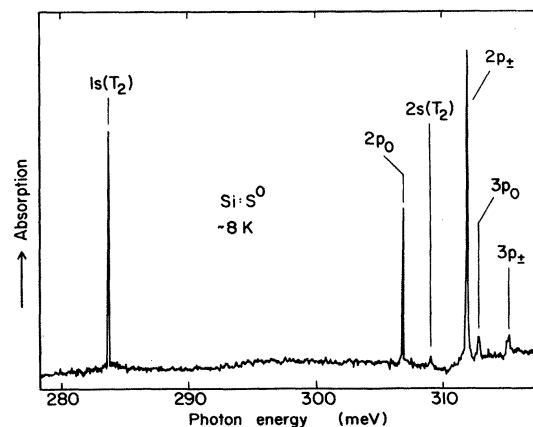


FIG. 5. Absorption spectrum of $Si:S^0$. The resolution is 0.12 meV.

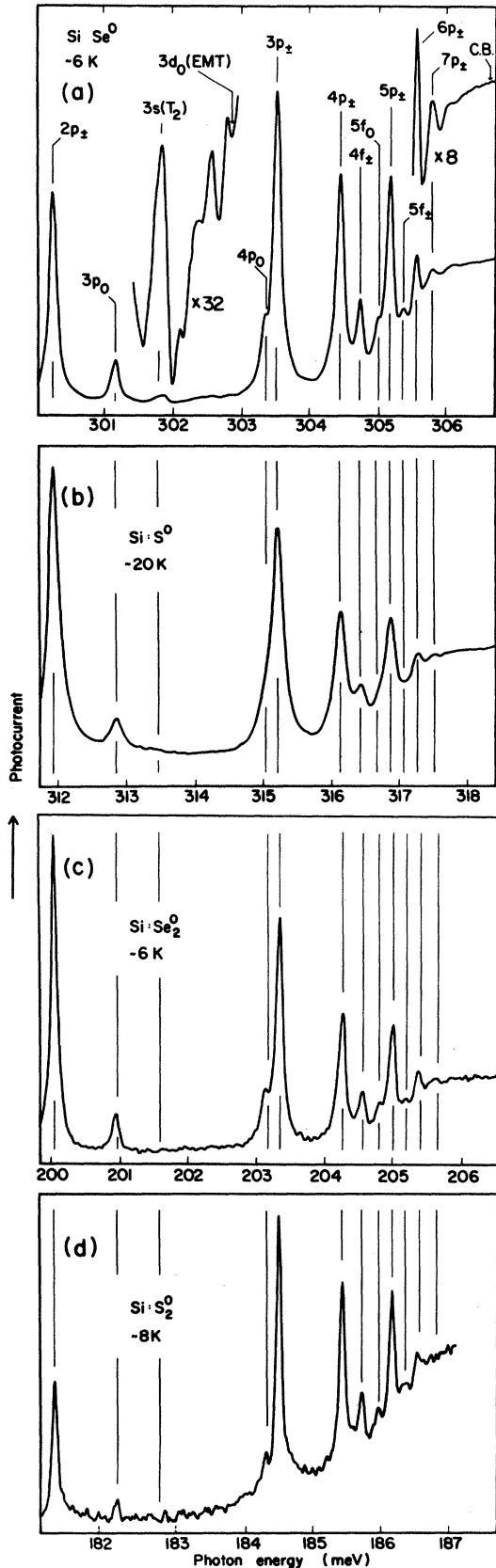


FIG. 6. Photoconductivity spectra showing the high-energy part of the spectrum for (a) Si:Se⁰, 0.03-meV resolution, with two magnified insets; (b) Si:S⁰, 0.06-meV resolution; (c) Si:Se₂⁰, 0.03-meV resolution; (d) Si:S₂⁰, 0.03-meV resolution.

valley coupling via the impurity potential is appreciable, each s -like EMT state splits into components with these labels; see Fig. 7(a). Characterizing these components by their transformation properties under symmetry operations, one finds that the A_1 , T_2 , and E states transform as spherical harmonics with $l=0, 1$, and 2 , respectively. Intervalley coupling depends on the amplitude of the EMT envelope wave function close to the center, and is strongest for s states, particularly so for $1s$. Only the A_1 component of the symmetry-coupled EMT states has a non-vanishing amplitude at the center, and it is, therefore, more affected by the local potential than the other two components. For the substitutional group-V donors,²⁰ as well as for the ionized chalcogen donors (D^+),⁹ it has been shown using ESR that the A_1 state is the ground state.

Within EMT, treating the defect as a screened point charge and considering only one valley of the conduction band, optical transitions from the ground state to s -like states are not allowed; see Fig. 3. The deeper the ground state, the more this selection rule will be relaxed. Strict selection rules governing the transitions between multivalley components are determined by the local symmetry of the defect. It will be seen from Figs. 4 and 5 that transitions to s -like states indeed become allowed for deep centers, and it is worth noting that the EMT-forbidden, but symmetry-allowed, transition to $1s(T_2)$ is even stronger than the EMT-allowed transition to $2p_0$ for the Se⁰ and S⁰ centers. Closer examination of the integrated intensities of absorption lines shows that for both the Se⁰ and S⁰ centers the relative intensities of the three dominant lines [$1s(T_2)$, $2p_0$, and $2p_{\pm}$] are 1.3:1:2.5 within the margin of error, which is about 10%.

Transitions from the ground state to $ns(E)$ and $ns(A_1)$ states are symmetry forbidden, and are in fact not observed even as very weak lines. But transitions to $1s(E)$ and $2s(A_1)$ can be observed indirectly through a higher-order process which involves a phonon and leads to Fano resonances (see Refs. 13 and 14). When the binding energies of $1s(E)$ and $2s(A_1)$ have been determined in this indirect manner, those of higher $ns(E)$ and $ns(A_1)$ states can be inferred by the following scaling procedure.

If the valley-orbit-split levels remain close to the corresponding EMT value, then the valley-orbit splitting scales approximately as $|F_{ns}(0)|^2$.²¹ Assuming the EMT envelope function $F_{ns}(r)$ varies with n as a hydrogenic wave function, the splitting for any n can be estimated once it is known for some n . The relative splittings for s states with $n=1, 2$, and 3 would then scale as $1:\frac{1}{8}:\frac{1}{27}$. From Table II it can be seen that the binding energies of $1s(E)$ for both the S⁰ and Se⁰ centers are close to the EMT $1s$ value, and those of $1s(T_2)$ are almost as close, so we may expect the scaling formula to apply to $ns(E)$ - $ns(T_2)$ pairs. For instance, the splitting for the $1s$ pair (compare Table II) of the Se⁰ center is 3.2(4) meV. By taking the binding energies of the T_2 states from experiment, the predicted binding energies of the $2s(E)$ and $3s(E)$ states are 8.87 and 4.78 meV, respectively. It may be noted that all $ns(E)$ levels are close to the EMT, which may be compared with the fact that E orbitals, transforming as $l=2$ spherical harmonics, are "pushed" farther out from the origin than

TABLE II. Experimentally determined binding energies for neutral centers (meV), compared with the EMT values given by Faulkner (see Ref. 3) and EMT values obtained in the present work. Values marked with w are weak lines, and those marked with a ? are questionable designations.

	EMT (Ref. 3)	EMT (Present work)	S ⁰	Se ⁰	S ₂ ⁰	Se ₂ ⁰	S _c ⁰ (X ₁)	S _c ⁰ (X ₂)	S _c ⁰ (X ₃)
1s(A ₁ ⁺)	31.27	31.262	318.32	306.63	187.61	206.44	109.52	92.00	82.16
1s(T ₂)(E ⁻)			34.62	34.44	31.26	31.30			
(A ₁ ⁻)					26.46	25.72			
1s(E ⁺)			31.6 ^a	31.2 ^a	34.4 ^a	33.2 ^a			
2s(A ₁ ⁺)	8.83	8.856	18.4 ^a	18.0 ^a	15.3 ^a	15.9 ^a			
2p ₀	11.51	11.492	11.48	11.49	11.49	11.58	11.62 ^b		
2s(T ₂)(E ⁻)	8.83	8.856	9.22	9.27	8.86	8.86	9.98?	10.01?	
(A ₁ ⁻)					8.21	8.11	...	8.36?	
2s(E ⁺)			9.62?	9.24?			
2p _±	6.40	6.402	6.39	6.39	6.39	6.39	6.38	6.40	6.40
3p ₀	5.48	5.485	5.45 ^b	5.48 ^b	5.48 ^b	5.51 ^b	5.48
3s	4.75	4.777	4.88	4.90	4.8(E ⁻)	...	4.8w ^b
					4.5(A ₁ ⁻)				
3d _±	...	3.874							
3d ₀	3.75	3.751	...	3.80	3.92 ^b	3.89 ^b	3.8w ^b
4p ₀	3.33	3.309	3.31	3.29 ^w	3.29	3.31
3p _±	3.12	3.120	3.12	3.12	3.12	3.12	3.12	3.12	3.12
4s	2.85	2.911	2.84?	2.81?
3d _{±2}	...	2.632							
4f ₀	2.33	2.339
4p _±	2.19	2.187	2.19	2.20	2.18	2.19	2.19	2.20	2.18
4f _±	1.89	1.894	1.91	1.90	1.89	1.89	1.89	...	1.91
5f ₀	1.62	1.630	1.65 ^b	1.63w ^b	1.67 ^b	1.64 ^b	1.67w
5p _±	1.44	1.449	1.46	1.46	1.46	1.46	1.46	1.47	1.46
5f _±	1.27	1.260	1.28	1.26	1.26	1.27	1.28
6h ₀	1.10	1.102							
6p _±	1.04	1.070	1.08	1.08	1.08	1.08			
6f _±	0.98	1.002							
6h _±	0.88	0.886							
7p _±		0.822	0.82 ^b	0.85	0.86 ^b	0.82 ^b			

^aLess accurate results (from Ref. 14).

^bLess accurate results.

the corresponding A₁ and T₂ orbitals.

Applying the scaling procedure to the A₁-T₂ splitting of 2s and 3s states—it is not valid for 1s states, since 1s(A₁) differs too much from the EMT—we find the binding energy of 3s(A₁) to be 7.5 meV for the Se⁰ center. However, the scaling procedure may not be reliable for 3s states, since their variational EMT envelope function contains an appreciable admixture of other than 3s basis functions. Taking the envelope function from our calculation (Sec. III), we do, nevertheless, find very similar scaling factors. It may be remarked that the observed strengths and energies of 3s transitions varied somewhat in our sam-

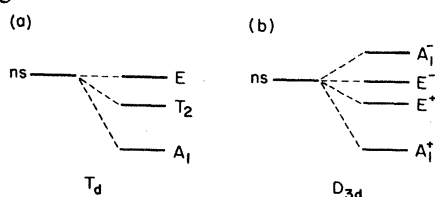


FIG. 7. Valley-orbit splitting of EMT ns levels for T_d and D_{3d} symmetries.

ples, and that the figures quoted in Table II are from samples where the $3d_{(0,\pm)}$ transitions were scarcely discernible (see below).

It will be seen in the left-hand inset of Fig. 6(a), showing a photoconductivity spectrum of the Se⁰ center, that there are four weak peaks corresponding to binding energies of 3.84, 4.07, 4.30, and 4.53 meV between the 3s(T₂) peak and the arrow marked "3d₀(EMT)." It is not clear what they are—they may be derived solely from 3d₀, or may be partly derived from 3d_± (see also Ref. 24 in Ref. 22). Spin-valley splitting could conceivably produce four components from 3d₀ and 3d_±, but as the splitting and shift relative to the EMT 3d₀ are rather large, and as no analogous effect is seen for other lines, this explanation is dubious. For Fig. 6(a) the field was less than 10 V/cm and the Se concentration about $3 \times 10^{15} \text{ cm}^{-3}$. For Fig. 4(a), an absorption spectrum for the same center, the concentration of Se was $3 \times 10^{16} \text{ cm}^{-3}$. There, the four peaks (positions indicated by arrows in the inset) are not visible, but nearby there is a well-defined peak close to the EMT value for 3d₀. This latter peak is the source for the 3d₀

binding energy quoted in Table II. A similar peak seems to occur in Si:S^0 , but it is not certain enough to be included in the table.

VI. D_2^0 SPECTRA

Since the spectra of the S_2^0 and Se_2^0 centers are similar, as are also those of the S_2^+ and Se_2^+ centers, the sites occupied by S pairs and Se pairs must be the same. The symmetry of the S_2^0 center was shown by Krag *et al.*²³ to be trigonal ($\langle 111 \rangle$ axis), i.e., C_{3v} , or, if there is a center of inversion, D_{3d} . Ludwig²⁴ found that the atoms in the S_2^+ pair are on close, equivalent sites, which is consistent with trigonal symmetry; also see Camphausen *et al.*, Ref. 25. Our results, particularly the absence of direct transitions to E^+ states, which can be detected indirectly via their phonon replicas (see below), indicate D_{3d} symmetry. Trigonal symmetry implies that a D_2 pair lies along an axis through a nearest-neighbor pair in the host lattice, and along such an axis there are two centers of inversion in each unit cell—one midway between nearest neighbors and another a distance $2d$ from the first (where d is the nearest-neighbor distance). Any D_2 pair symmetrically disposed about such a center will have D_{3d} symmetry, but the most likely configuration is a substitutional pair on nearest-neighbor sites. We cannot, however, exclude the second possibility, that the D_2 pair occupies the two "empty sites" on either side of the second center of inversion. Since the effective Bohr radius of shallow donors in silicon is about an order of magnitude larger than the nearest-neighbor distance, we assume that we may still view the D_2 center as a simple donor with excited states given rather accurately by the EMT. In fact, a sphere containing both impurity atoms on nearest-neighbor sites contributes only about 10^{-6} to the norm of the $2p_0$ envelope functions.

The point group D_{3d} may be regarded as the direct product of the point groups C_{3v} and C_i , where the latter contains the identity and the inversion operation. The basis functions for irreducible representations of D_{3d} can thus be classified according to their transformation properties under C_{3v} (A_1 , A_2 , and E) (Ref. 26) and their parity, which we here indicate by a superscript + or -. Figure 7(b) illustrates the valley-orbit splitting of sixfold-degenerate s -like EMT states into A_1^+ , E^+ , E^- , and A_1^- components of D_{3d} . The ground state $1s(A_1^+)$ has an antinode at the center, and is much deeper than any other state. A_1^+ states here are obtained by the same linear combination of single-valley states as the A_1 states in T_d symmetry, and E^+ states are obtained by the same combinations as the E states of T_d symmetry. The electric dipole transition operator decomposes into components transforming as A_1^- and E^- . Transitions from the ground state $1s(A_1^+)$ are thus only allowed to A_1^- and E^- states. Regarding the order of symmetry-split components, it has been shown by the application of uniaxial stress that the highest $1s$ state in S_2^0 -center absorption is a singlet, and the other a doublet.²³ From its observation in phonon replica as a Fano resonance^{13,14} we find that the $1s(E^+)$ state lies below both optically allowed final states. As already mentioned, the absence of direct optical transi-

tions to this state allow its parity to be determined. We thus arrive at the ordering A_1^+ , E^+ , E^- , and A_1^- , and assume that this order applies for all split s states of the S_2^0 , Se_2^0 , S_2^+ , and Se_2^+ centers in this paper. One might have expected the A_1^- state to be highest, since, in a molecular picture, it would correspond to a state made up of anti-bonding s orbitals, with the node at the origin inducing rapid variations of the total wave function.

The split s states of the S_2^0 and Se_2^0 centers are shown in Figs. 8 and 9, and the results for the upper $1s$ levels are summarized in Fig. 10.²⁷ The $1s(E^-)$ level is closest to the EMT value. Hence, the $2s(E^-)$ and $3s(E^-)$ levels can be assigned by comparison with the EMT values, and the other $2s$ and $3s$ levels can be assigned or estimated using the same scaling argument as before. The results are shown in Table III. The simple combination of the EMT and scaled splitting agrees well with the observations.

The $2s(A_1^-)$ line was visible in most samples, whereas the $2s(E^-)$ line was sometimes broad and rather uncertain in position. For some samples there was a slightly deeper level (see, for instance, the left-hand inset of Fig. 8). This has been included in Table III in parentheses under the label $2s(E^+)$. This label seems to be the only one available, and might apply if some factor such as a local electric field were to weaken the selection rule forbidding transitions to such a state. As the table shows, this assignment is not in good agreement with the prediction from scaling.

The p -like levels of the S_2^0 and Se_2^0 centers were not split, and their energies agree closely with the EMT, as may be seen in Table II. The ratio of the integrated intensity of the $2p_{\pm}$ line to that of the $2p_0$ line (the two strongest lines) was 2.4 ± 0.2 in both cases, which is similar to the ratio obtained for the S^0 and Se^0 centers.

VII. NEUTRAL SULFUR-RELATED COMPLEXES $\text{S}_c^0(X_i)$

The binding energies of four neutral and two ionized complexes related to sulfur and selenium are given in Figs.

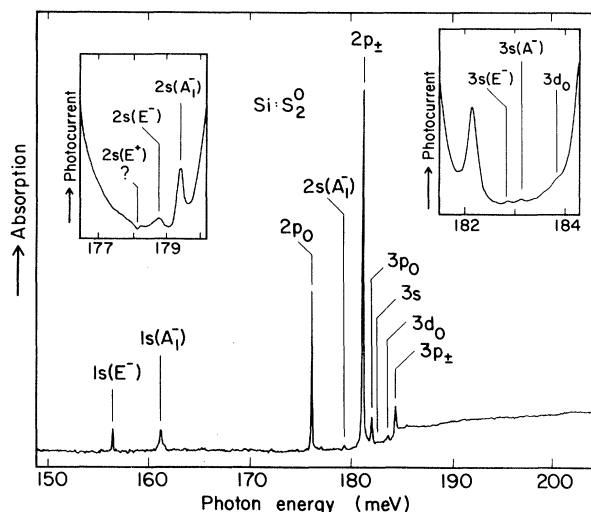


FIG. 8. Absorption spectrum of Si:S_2^0 showing the split s states. The resolution is 0.12 meV. The insets are from photoconductivity measurements of different samples at higher temperatures and using appropriate optical filters.

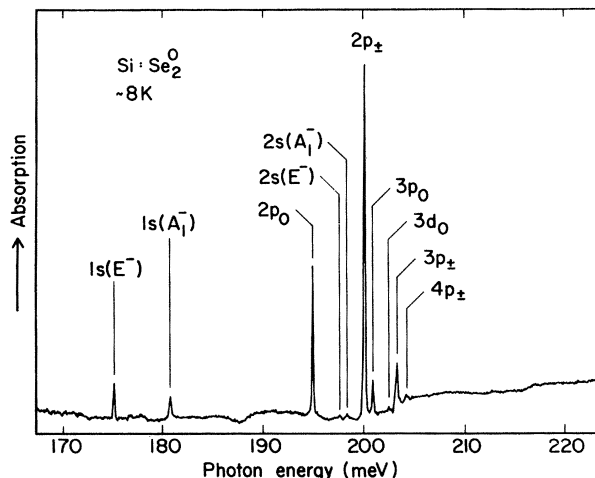


FIG. 9. Absorption spectrum of $\text{Si}:\text{Se}_2^0$ at 0.12-meV resolution.

1 and 2. These centers have all been observed by us, though details for the $\text{Se}_c^0(X_1)$ center are not presented here because only its $2p_0$, $2p_{\pm}$, and $3p_{\pm}$ transitions were discernible.

The $\text{S}_c^0(X_1)$ center was reported as the “A center” by Krag *et al.*²³ The analogous center for selenium and its ionized version, $\text{Se}_c^+(X_1)$, were observed by Swartz *et al.*²⁸ The centers $\text{S}_c^0(X_2)$ and $\text{S}_c^0(X_3)$, together with some other sulfur-related complexes, have been reported in a private communication from Wagner *et al.*²⁹ Brotherton *et al.*³⁰ recently reported shallow centers in sulfur-doped silicon which varied with the substrate and fabrication procedure, one of them, the “Z level” with binding energy 0.08 eV, being similar to $\text{S}_c^0(X_3)$. Complexes X_1 and X_3 derived from magnesium-doped silicon and with binding energies close to those of $\text{S}_c^0(X_2)$ and $\text{S}_c^0(X_3)$ were recently reported by Lin,⁷ together with two shallow donor centers. It seems probable that whole series of centers related to sulfur and selenium and closely spaced in binding energy can be produced by varying the diffusion temperature and annealing treatment. There is an evident analogy here to the series of “thermal donors” related to oxygen,^{4–6} the group companion in the Periodic Table.

Figure 11 shows photoconductivity spectra of the $\text{S}_c^0(X_1)$ and $\text{S}_c^0(X_3)$ complexes. Similar absorption spectra have been reported earlier by Krag *et al.*,²³ although they interpreted the $\text{S}_c^0(X_3)$ lines as being $1s$ levels of $\text{S}_c^0(X_1)$.

TABLE III. Comparison between experimental and predicted values for s states of S_2^0 and Se_2^0 centers. Predicted values are from the EMT, with empirically estimated valley-orbit splitting as described in the text. Similar experimental results for the $2s$ (E^- and A_1^-) and $3s$ (E^- and A_1^-) states of $\text{Si}:\text{S}_2^0$ are found in Ref. 22.

	A_1^+		E^+		E^-		A_1^-		
	$\text{Si}:\text{S}_2^0$	$\text{Si}:\text{Se}_2^0$	$\text{Si}:\text{S}_2^0$	$\text{Si}:\text{Se}_2^0$	$\text{Si}:\text{S}_2^0$	$\text{Si}:\text{Se}_2^0$	$\text{Si}:\text{S}_2^0$	$\text{Si}:\text{Se}_2^0$	$\text{Si}:\text{Se}_2^0$
1s expt.	187.61	206.44	34.4	33.2	31.26		31.30	26.46	25.72
2s pred.			9.25	9.09		8.856		8.26	8.16
2s expt.	15.3	15.9	(9.62)	(9.24)	8.86		8.86	8.21	8.11
3s pred.	6.68	6.86	4.89	4.85		4.777		4.60	4.57
3s expt.					4.8			4.5	

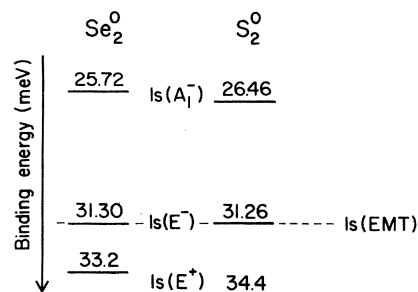


FIG. 10. Experimentally determined binding energies of the nearly EMT-like $1s$ states of Se_2^0 and S_2^0 centers. The $1s(A_1^-)$ and $1s(E^-)$ levels have been obtained from no-phonon absorption or photoconductivity. The $1s(E^+)$ states are only seen as Fano resonances above the ionization limit.

However, the four lines they reported do correspond to the $2p_0$, $3p_{\pm}$, $4p_{\pm}$, and $5p_{\pm}$ levels of the $\text{S}_c^0(X_3)$ center, and the fact that they did not see the strong $2p_{\pm}$ line was probably due to its close proximity to the strong carbon absorption line. Figure 11 clearly shows that there are two different centers.

The sample used for the photoconductivity measurement in Fig. 11 was subject to diffusion at 1100°C. At lower temperatures the $\text{S}_c^0(X_2)$ center appears—see Fig. 12. All our data on neutral complexes are summarized in Table II.

VIII. D^+ AND D_2^+ CENTERS

Spectra of the S^+ and Se^+ centers are not given here since equally good spectra have been published earlier.^{22,23,28,31} We confine ourselves to a few remarks. Our result for the binding energy of the Se^+ -center $1s(A_1)$ state is 593.3 meV, in agreement with Ref. 31, but not with the 589.4-meV value of Ref. 28. The broadening of the $2s(T_2)$ line for the Se^+ center (binding energy 39.3 meV) is probably due to spin-valley splitting.³¹ From the splitting of the $1s(T_2)$ state and the scaling procedure described earlier, the splitting of the $2s(T_2)$ line is estimated to be 0.3 meV.

Absorption spectra of the S_2^+ and Se_2^+ centers are shown in Figs. 13 and 14. It is assumed that the A_1^- component of s states has higher energy than the E^- component, by analogy to the S_2^0 center. Where overlapping with spectra of other centers occurs this is indicated in the figure. There has been no difficulty in separating lines

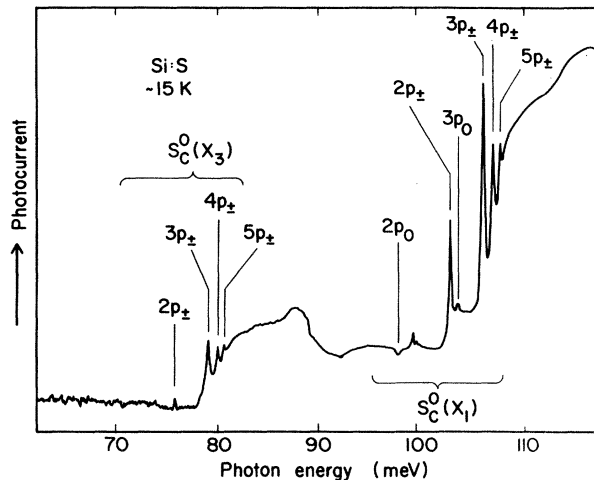


FIG. 11. Photoconductivity spectrum of sulfur-doped silicon showing line spectra of two different centers, $S_c^0(X_1)$ and $S_c^0(X_3)$. The peak at 99.5 meV has not been reported previously and is of unknown origin. It may be a $2s$ level. The resolution is 0.12 meV.

from different centers, even when they lie as close together as in Fig. 13, since we have data for other samples where either the one center or the other is absent.

The line spectra of D_2^+ are not described as extremely well by the EMT as those of D^+ or, in particular, D_2^0 and D^0 . The binding energies are nevertheless obtained here by taking the $3p_{\pm}$ state to be $4 \times 3.12 = 12.48$ meV—the EMT value—below the conduction band. For the ground states the results are 371.1 meV for the S_2^+ center and 389.5 meV for the Se_2^+ center. Actually, the $3p_{\pm}$ level of these centers is probably deeper than the EMT estimate. If the $4p_{\pm}$ level were used instead in deriving the ground-state binding energy, the binding energy would be larger by about 0.2 meV. Such a change in the ground-state energy would of course affect the $1s$ binding energies given

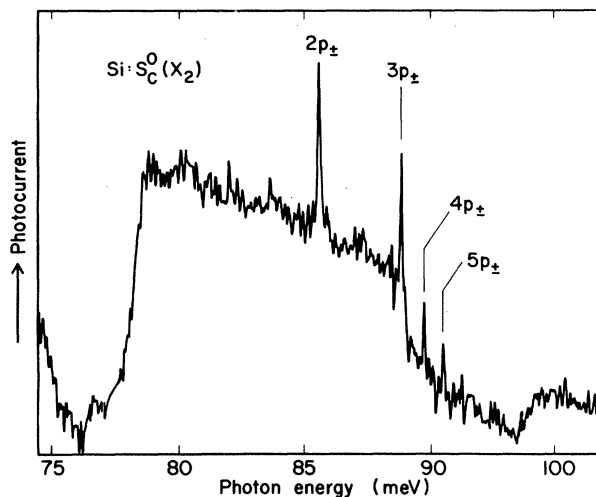


FIG. 12. Photoconductivity spectrum of sulfur-doped silicon showing the line spectrum of $S_c^0(X_2)$. The resolution is 0.06 meV.

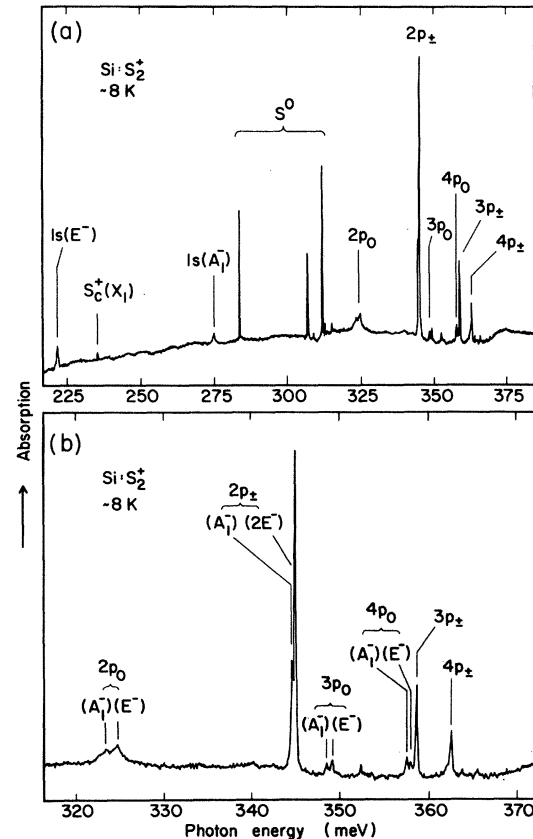


FIG. 13. (a) Absorption spectrum of sulfur-doped silicon showing mainly the S_2^+ center. The resolution is 0.24 meV. (b) Enlarged part of (a) showing only the higher excited S_2^+ -center lines.

in Fig. 15 and the $2p$ energies in Fig. 17, but not the relative energies.

There are little data for s states. The assignments for $2s$ states are tentative, the $1s$ assignments firmer; see Fig. 15. It is worth noting that the only large difference between

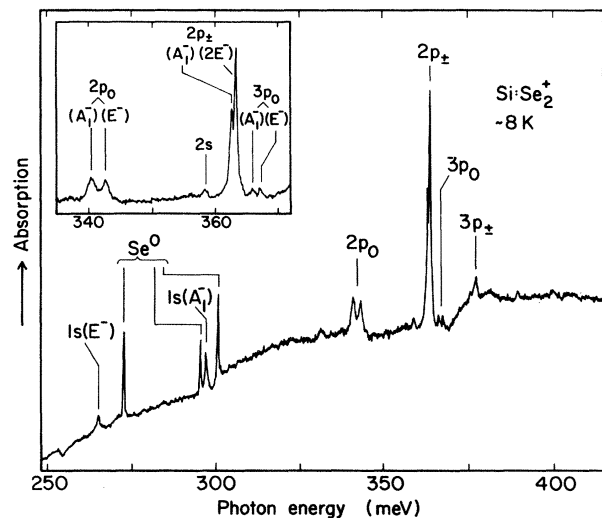


FIG. 14. Absorption spectrum of selenium-doped silicon showing mainly the Se_2^+ center. The resolution is 0.06 meV.

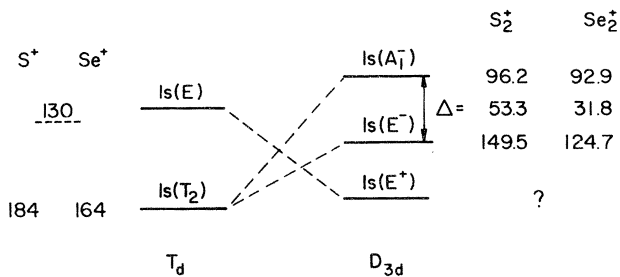


FIG. 15. Comparison between the binding energies (in meV) of excited $1s$ states for D^+ (T_d symmetry) and D_2^+ (D_{3d} symmetry). The energies are experimental except for the $1s(E)$ T_d state (dashed), which is as calculated by Altarelli (see Ref. 32). Neither this state nor the $1s(E^+)$ state have been observed experimentally, but they are assumed to behave like the corresponding neutral states.

binding energies in the S_2^+ and Se_2^+ centers is for the $1s(E^-)$ state, which is 25 meV deeper in the S_2^+ center. This may be compared with the result for the deepest excited state in the S^+ and Se^+ centers, $1s(T_2)$, which is 20 meV deeper in S^+ (cf. Fig. 15). For the Se_2^+ center—as for D_2^0 (see Fig. 10)—the $1s(E^-)$ state is close to the EMT position, 125 meV below the conduction band. Comparing the $1s(A_1^-)$ - $1s(E^-)$ splittings of D_2^+ and D_2^0 , we note that the results agree roughly with the expectation that they should scale as Z^3 . The $1s(E^-)$ state in the S_2^+ center is split (about 0.6 meV), probably due to spin-valley interaction, like the $1s(T_2)$ state of the S^+ , Se^+ , and Te^+ ,³¹ see Fig. 16. Our samples containing Se_2^+ centers gave a $1s(E^-)$ line which was too broad for any similar splitting to be observable there. We have no evidence that the $1s(E^+)$ state of D_2^+ will behave as shown in Fig. 15, but we assume a similar behavior as for D_2^0 . The energy position of the $1s(E)$ T_d state—130 meV—has been calculated by Altarelli³² but has not been observed experimentally.

It is found experimentally that all p lines with binding energies greater than about 13 meV are split by valley-

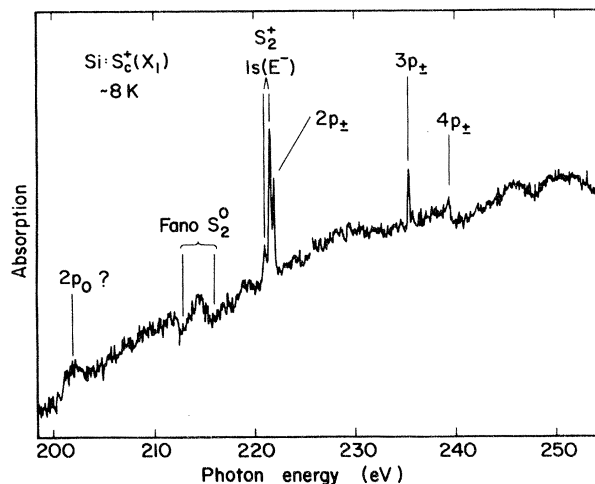


FIG. 16. Absorption spectrum of sulfur-doped silicon showing the line spectrum of the $S_c^+(X_1)$ complex and the split $1s(E^-)$ line belonging to the S_2^+ center.

orbit interaction, more so for the Se_2^+ center than for S_2^+ , and more so for p_0 than for p_{\pm} ; see Figs. 13, 14, and 17. The splittings are 1.36, 0.33, 0.64, and 0.46 meV, respectively, for the $2p_0$, $2p_{\pm}$, $3p_0$, and $4p_0$ states of the S_2^+ center and 2.27, 0.71, and 1.03 meV, respectively, for the $2p_0$, $2p_{\pm}$, and $3p_0$ states of the Se_2^+ center. The uncertainties in these values are rather large, about 0.05 meV.³³ It may be remarked that there is no discernible shift or splitting of p states in S^+ and Se^+ centers, which have binding energies close to the EMT value in both cases. This indicates that the much less symmetric central region of the impurity potential in D_2^+ exercises a greater intervalley perturbation on EMT states. Comparing D_2^+ and D_2^0 , we note that the squared amplitudes of hydrogenic p states scale as Z^5 near the origin. Reducing the splittings of D_2^+ by this factor, one would expect the corresponding splittings of D_2^0 to be, at most, 0.07 meV ($Se_2^0:2p_0$), and thus remain unresolved in the samples available for the present work.

In D_{3d} symmetry the six p_0 states split, in the manner of the s -like states, into A_1^+ , A_1^- , E^+ , and E^- components, whereas the 12 p_{\pm} states split into A_1^+ , A_1^- , A_2^+ , A_2^- , two E^+ , and two E^- components. From the ground state $1s(A_1^+)$ only transitions to A_1^- and E^- states are allowed, and only these allowed levels are included in Figs. 15 and 17.

The p_0 lines may thus split into two lines, as is observed experimentally, while of the three possible p_{\pm} lines two remain too close to be resolved experimentally. The p -like levels are shown schematically in Fig. 17, where the symmetry assignment for the D_{3d} states is somewhat tentative. The A_1^- states can be viewed as p -type orbitals oriented along the [111] direction, whereas the corresponding p orbitals are orthogonal to the impurity-pair axis for the E^- states. One may then expect the A_1^- states oriented along the defect axis to be more strongly perturbed by the attractive "central-cell" potential of the impurity pair.

The fact that the splitting is larger for p_0 components than for p_{\pm} is probably due to the larger amplitude of p_0 states in the central region of the impurity potential, depending on the fact that $m_l \approx 5m_t$. A modified scaling

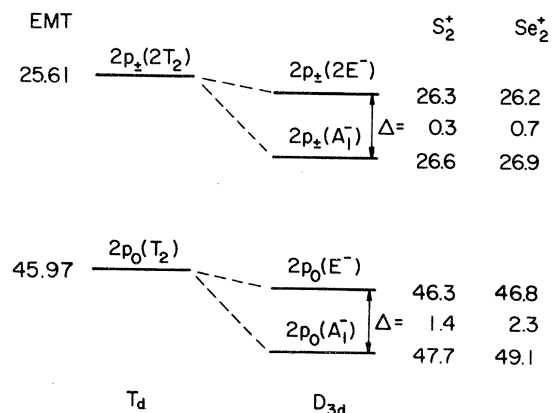


FIG. 17. Components of $2p_0$ and $2p_{\pm}$ states split by valley-orbit interaction which are allowed as final states in no-phonon absorption. Results for D_{3d} symmetry (S_2^+ and Se_2^+ centers) are compared with those for T_d symmetry (S^+ and Se^+ centers). The latter states are close to the EMT position.

procedure can be applied here, now using the term proportional to r in the radial distribution. The EMT envelope functions for the three lowest p_0 states are shown by our calculation to be reasonably "pure," i.e., the variational wave function is almost entirely given by the corresponding np_0 trial basis function. We find that the squared amplitudes of the p_0 states at the center of either impurity atom scale as 1.0:0.59:0.36 for $2p_0$, $3p_0$, and $4p_0$. Experimentally, we find the corresponding relative splitting to be 1.0:0.47:0.34 for S_2^+ centers and 1.0:0.45 for Se_2^+ centers in satisfactory agreement with the theoretical prediction.

While the two p_0 components are of about the same intensity, the upper component of the $2p_{\pm}$ lines is much stronger than the lower. By assuming the transition probability to A_1^- and E^- to be approximately equal, the intensity ratios can be understood on the basis of the tentative assignments of Fig. 17, according to which the degeneracy of the upper $p_{\pm}(2E^-)$ level is twice that of the upper $p_0(E^-)$ level. The integrated intensity of the $2p_{\pm}$ pair of lines is approximately 2.0 times that of the $2p_0$ pair for both S_2^+ and Se_2^+ centers, which, considering the rather large margins of error for such ratios, is not very different from what was found for these states in S^0 , Se^0 , S_2^0 , and Se_2^0 centers.

Another noteworthy effect is that the $2p_0$ lines of S_2^+ and Se_2^+ centers are considerably broader than any other lines in these spectra. This is not so for the $2p_0$ lines in S^+ and Se^+ centers, which have about the same binding energy, nor is it so for the $2p_0$ lines in S_2^0 and Se_2^0 centers, which have the same symmetry. [The line assigned $2p_0$ of the $S_c^+(X_1)$ center reported in Sec. IX is also broad, but too little is known about this center and its spectrum to include it in the present discussion.] The anomalous broadening of the $2p_0$ lines may be explained as a lifetime effect, the $2p_0$ states decaying to lower excited states via intervalley phonons. The f LA phonon in silicon has an energy of about 46 meV,³⁴ while the energy difference between $2p_0$ and $1s(A_1^-)$ is ~ 49 meV in the S_2^+ center and ~ 45 meV in the Se_2^+ center. An analogous case occurs for Bi in silicon,^{35,36} where one observes this resonant in-

teraction between the f TO phonons and the transition from the $1s(A_1)$ ground state to the $2p_0$ state.

IX. $S_c^+(X_1)$ CENTER

The $2p_{\pm}$, $3p_{\pm}$, and $4p_{\pm}$ lines of a center that has not been reported previously can be seen in Fig. 16. The binding energy is 247.9 meV. A broad line identified as $2p_0$ has also been observed. The corresponding center for selenium has been reported earlier.²⁸ The center could be $S_c^+(X_1)$, i.e., the ionized version of $S_c^0(X_1)$.

X. SUMMARY

Absorption and photoconductivity spectra have been obtained for a number of Si:S and Si:Se samples prepared under varying conditions to favor the production of different centers. Spectra for seven sulfur-related centers and three selenium-related centers are presented in figures and tables of the binding energies of observed levels, together with details of line splitting and other features of interest. Comparison is made with experimental results of others, and with a new calculation of binding energies according to the EMT. Splitting of states due to intervalley interaction is compared with a model based on simple estimates of wave functions near the origin, where the effect of local symmetry is strong. Anomalous broadening of the $2p_0$ line in the spectra of S_2^+ and Se_2^+ centers is explained in terms of decay to a lower excited state via intervalley phonons. Full interpretation of the lowest levels and of valley-orbit splitting awaits the development of better methods for calculating the electronic structure of deep levels.

ACKNOWLEDGMENTS

We are indebted to P. Wagner for valuable discussions and to M. Ahlström and C. Holm for sample preparation. We also thank K. Larsson for help with spectral measurements.

*Present address: Optical Sensors Innovation Department, ASEA Innovation, S-721 83 Västerås, Sweden.

¹H. G. Grimmeis and E. Janzén, in *Defects in Semiconductors*, Proceedings of the Material Research Society's annual meeting, 1982 (in press).

²H. G. Grimmeis, in *Electrochemical Society Symposium on Aggregation Phenomena of Point Defects in Silicon*, München, 1982 (in press).

³R. A. Faulkner, *Phys. Rev.* **184**, 713 (1969).

⁴D. Wruck and P. Gaworzewski, *Phys. Status Solidi A* **56**, 557 (1979).

⁵B. Pajot, H. Compain, J. Lerouille, and B. Clerjaud, in *Proceedings of the 16th International Conference on the Physics of Semiconductors, Montpellier, 1982*, edited by M. Averous (North-Holland, Amsterdam, 1983), p. 110.

⁶R. Oeder and P. Wagner, in *Defects in Semiconductors*, Ref. 1.

⁷A. Lin, *J. Appl. Phys.* **53**, 6989 (1982).

⁸N. Sclar, *J. Appl. Phys.* **52**, 5207 (1981).

⁹H. G. Grimmeis, E. Janzén, H. Ennen, O. Schirmer, J.

Schneider, R. Wörner, C. Holm, E. Sirtl, and P. Wagner, *Phys. Rev. B* **24**, 4571 (1981).

¹⁰These samples were fabricated by Dr. C. Holm at Heliotronic.

¹¹G. Arfken, *Mathematical Methods for Physicists* (Academic, New York, 1970), p. 620.

¹²The new EMT calculations presented here give us a tentative explanation for the split " $3d_0$ " states observed for P^0 and Bi^0 centers (see Ref. 16 and references therein)—the splitting being about 0.1 meV. The two closely spaced lines could be transitions to the $3d_{\pm}$ and $3d_0$ states, which are 0.12 meV apart.

¹³E. Janzén, R. Stedman, and H. G. Grimmeis, in *Proceedings of the 16th International Conference on the Physics of Semiconductors, Montpellier, 1982*, Ref. 5, p. 125.

¹⁴E. Janzén, G. Grossmann, R. Stedman, and H. G. Grimmeis (unpublished).

¹⁵R. G. Humphreys, P. Migliorato, and G. Fortunato, *Solid State Commun.* **40**, 819 (1981).

¹⁶B. Pajot, J. Kaupinnen, and R. Antilla, *Solid State Commun.*

- 31, 759 (1979).
- ¹⁷C. Jagannath, Z. W. Grabowski, and A. K. Ramdas, *Phys. Rev. B* **23**, 2082 (1981).
- ¹⁸M. S. Skolnick, L. Eaves, R. Stradling, J. C. Portal, and S. Askenazy, *Solid State Commun.* **15**, 1403 (1974).
- ¹⁹W. Kohn and J. M. Luttinger, *Phys. Rev.* **98**, 915 (1955).
- ²⁰G. Feher, *Phys. Rev.* **114**, 1219 (1959).
- ²¹F. Bassani, G. Iadonisi, and B. Preziosi, *Rep. Prog. Phys.* **37**, 1099 (1974).
- ²²W. H. Kleiner and W. E. Krag, *Phys. Rev. Lett.* **25**, 1490 (1970).
- ²³W. E. Krag, W. H. Kleiner, H. J. Zeiger, and S. Fischler, *J. Phys. Soc. Jpn. Suppl.* **21**, 230 (1966).
- ²⁴G. W. Ludwig, *Phys. Rev.* **137**, A1520 (1965).
- ²⁵D. L. Camphausen, H. M. James, and R. J. Sladek, *Phys. Rev. B* **2**, 1899 (1970).
- ²⁶M. Tinkham, *Group Theory and Quantum Mechanics* (McGraw-Hill, New York, 1964), Appendix B.
- ²⁷Recently, P. Wagner (see Ref. 29) observed the Te_2^0 center in absorption. The $1s(A_1^-)$ state is 25.8 meV and the $1s(E^-)$ state 33.1 meV below the conduction band. Also see E. Sirtl, Electrochemical Society, Spring Meeting, 1983 (unpublished).
- ²⁸J. C. Swartz, D. H. Lemmon, and R. N. Thomas, *Solid State Commun.* **36**, 331 (1980).
- ²⁹P. Wagner (private communication).
- ³⁰S. D. Brotherton, M. J. Kling, and G. J. Parker, *J. Appl. Phys.* **52**, 4649 (1981).
- ³¹H. G. Grimmeiss, E. Janzén, and K. Larsson, *Phys. Rev. B* **25**, 2627 (1982).
- ³²M. Altarelli, in *Proceedings of the 16th International Conference on the Physics of Semiconductors, Montpellier, 1982*, Ref. 5, p. 122.
- ³³Splitting of p levels in S_2^+ and Se_2^+ centers has been reported previously (Refs. 22 and 28, respectively), but in less detail than here.
- ³⁴M. Asche and O. G. Sarbei, *Phys. Status Solidi B* **103**, 11 (1981).
- ³⁵A. Onton, P. Fisher, and A. K. Ramdas, *Phys. Rev. Lett.* **19**, 781 (1967).
- ³⁶N. R. Butler, P. Fisher, and A. K. Ramdas, *Phys. Rev. B* **12**, 3200 (1975).
- ³⁷R. O. Carson, R. N. Hall, and E. M. Pell, *J. Phys. Chem. Solids* **8**, 81 (1959).
- ³⁸C. T. Sah, T. H. Ning, L. L. Rosier, and L. Forbes, *Solid State Commun.* **9**, 917 (1971).
- ³⁹L. L. Rosier and C. T. Sah, *J. Appl. Phys.* **42**, 4000 (1971).
- ⁴⁰L. L. Rosier and C. T. Sah, *Solid State Electron* **14**, 41 (1971).
- ⁴¹O. Engström and H. G. Grimmeiss, *J. Appl. Phys.* **47**, 4090 (1976).
- ⁴²T. H. Ning and C. T. Sah, *Phys. Rev. B* **14**, 2528 (1976).
- ⁴³R. Y. Koyama, W. E. Phillips, D. R. Myers, Y. M. Liu, and H. B. Dietrich, *Solid State Electron* **21**, 953 (1978).
- ⁴⁴H. G. Grimmeiss, E. Janzén, and B. Skarstam, *J. Appl. Phys.* **51**, 4212 (1980).
- ⁴⁵F. Richou, G. Pelous, and D. Lecrosnier, *Appl. Phys. Lett.* **31**, 525 (1977).
- ⁴⁶H. R. Vydyanath, J. S. Lorenzo, and F. A. Kröger, *J. Appl. Phys.* **49**, 5928 (1978).
- ⁴⁷C. S. Kim, E. Ohta, and M. Sakata, *Jpn. J. Appl. Phys.* **18**, 909 (1979).
- ⁴⁸B. Skarstam and J. L. Lindström, *Appl. Phys. Lett.* **39**, 488 (1981).
- ⁴⁹H. G. Grimmeiss, E. Janzén, and B. Skarstam, *J. Appl. Phys.* **51**, 3740 (1980).
- ⁵⁰H. G. Grimmeiss and B. Skarstam, *Phys. Rev. B* **23**, 1947 (1981).